Optimal function of the DNA repair enzyme TDP1 requires its phosphorylation by ATM and/or DNA-PK

Benu Brata Das[1], Smitha Antony[1], Shalu Gupta[1], Thomas S Dexheimer[1], Christophe E Redon[1], Susan Garfield[2], Yosef Shiloh[3] and Yves Pommier[1,*]

[1]Laboratory of Molecular Pharmacology, Center for Cancer Research, National Cancer Institute, National Institutes of Health, Bethesda, MD, USA, [2]Laboratory of Experimental Carcinogenesis, Center for Cancer Research, National Cancer Institute, National Institutes of Health, Bethesda, MD, USA and [3]The David and Inez Meyers Laboratory for Cancer Genetics, Department of Human Molecular Genetics and Biochemistry, Sackler School of Medicine, Tel Aviv University, Tel Aviv, Israel

Human tyrosyl–DNA phosphodiesterase (TDP1) hydrolyzes the phosphodiester bond at a DNA 3′ end linked to a tyrosyl moiety. This type of linkage is found at stalled topoisomerase I (Top1)–DNA covalent complexes, and TDP1 has been implicated in the repair of such complexes. Here we show that Top1-associated DNA double-stranded breaks (DSBs) induce the phosphorylation of TDP1 at S81. This phosphorylation is mediated by the protein kinases: ataxia-telangiectasia-mutated (ATM) and DNA-dependent protein kinase (DNA-PK). Phosphorylated TDP1 forms nuclear foci that co-localize with those of phosphorylated histone H2AX (γH2AX). Both Top1-induced replication- and transcription-mediated DNA damages induce TDP1 phosphorylation. Furthermore, we show that S81 phosphorylation stabilizes TDP1, induces the formation of XRCC1 (X-ray cross-complementing group 1)–TDP1 complexes and enhances the mobilization of TDP1 to DNA damage sites. Finally, we provide evidence that TDP1–S81 phosphorylation promotes cell survival and DNA repair in response to CPT-induced DSBs. Together; our findings provide a new mechanism for TDP1 post-translational regulation by ATM and DNA-PK.

*Corresponding author. Laboratory of Molecular Pharmacology, Division of Basic Sciences, NIH, Center for Cancer Research, National Cancer Institute, Building 37, Room 5068, Bethesda, MD 20892-4255, USA. Tel.: + 1 301 496 5944; Fax: + 1 301 402 0752; E-mail: pommier@nih.gov

Introduction

Human tyrosyl–DNA phosphodiesterase (TDP1) typically hydrolyzes the phosphodiester bond between a DNA 3′ end and a tyrosyl moiety (Yang *et al*, 1996). In eukaryotes, 3′-tyrosyl–DNA adducts arise from the catalytic activity of DNA topoisomerase I (Top1), which relaxes positive DNA supercoiling ahead of replication forks and transcription complexes and can relax negative supercoiling behind such complexes. To that effect Top1 transiently cleaves one strand of duplex DNA by the nucleophilic attack of its active site tyrosine on the DNA phosphodiester backbone to yield a 3′ phosphotyrosyl bond (Champoux, 2001; Wang, 2002). The broken DNA strand with the free 5′ hydroxyl end then rotates around the non-scissile strand. The short-lived, covalent Top1–DNA cleavage complex (Top1cc) is readily reversed by a second transesterification reaction in which the 5′-hydroxyl end acts as a nucleophile to religate the DNA and to free Top1.

Top1cc intermediates can be converted into irreversible Top1–DNA cleavage complexes. Such DNA lesions trigger cell-cycle arrest and cell death (Pommier, 2006). Top1cc intermediates are selectively trapped by the plant alkaloid camptothecin (CPT) (Hsiang *et al*, 1985) as the drug binds at the enzyme–DNA interface and prevents DNA religation (Staker *et al*, 2005; Pommier, 2006). Top1cc intermediate can also be trapped by endogenous DNA lesions, including abasic sites, mismatches, UV and IR radiation-induced DNA damage, oxidized bases, nicks, and carcinogenic DNA adducts (Pourquier and Pommier, 2001; Pommier *et al*, 2006a). Hence, DNA modifications such as those associated with oxidative damage can stabilize Top1cc. Top1-linked DNA single-strand breaks can be subsequently transformed into DNA double-stranded breaks (DSBs) after collision with the replication and transcription machineries (Liu *et al*, 2000; Pommier *et al*, 2006a; Sordet *et al*, 2009). Thus, repairing irreversible Top1cc intermediate is an important part of DNA metabolism.

The ability of TDP1 to resolve 3′ phosphotyrosyl linkages is consistent with a role for the enzyme in protecting cells against cytotoxic Top1–DNA lesions. Homozygous mutation of TDP1 causes spinocerebellar ataxia with axonal neuropathy (SCAN1), an autosomal recessive neurodegenerative syndrome (Takashima *et al*, 2002). Cells from SCAN1 patients are hypersensitive to CPT and accumulate Top1-linked DNA breaks (El-Khamisy *et al*, 2005; Interthal *et al*, 2005b; Miao *et al*, 2006). TDP1 was originally discovered in yeast by screening mutagenized strains that lacked tyrosylphosphodiesterase activity (Pouliot *et al*, 1999; Dexheimer *et al*, 2008). TDP1 activity is not limited to the removal of cellular Top1 adducts; it can also process other 3′ DNA end blocking lesions: 3′ abasic sites and 3′ phosphoglycolate (Zhou *et al*, 2005; Interthal *et al*, 2005a; Hawkins *et al*, 2009). TDP1$^{-/-}$ cells are significantly deficient in removing 3′ phosphoglycolate at a DSB (Zhou *et al*, 2005, 2009; Hawkins *et al*, 2009).

TDP1 also possesses a limited DNA and RNA 3′ exonuclease activity during which a single nucleoside is removed from the 3′-hydroxyl end of the substrate (Interthal *et al*, 2005a). Thus, TDP1 may function to remove a variety of adducts from 3′ DNA ends during DNA repair of single- and double-strand breaks (Dexheimer *et al*, 2008).

In yeast, TDP1 and RAD52 act in the same epistasis group, which is indicative of a possible role for TDP1 in DSB repair (Pouliot *et al*, 2001). Recently, TDP1 has also been implicated in the repair of yeast topoisomerase II (Top2) cleavage complexes (Nitiss *et al*, 2006). Moreover, TDP1 overexpression in human cells counteracts DNA damage mediated not only by Top1 but also by Top2 (Barthelmes *et al*, 2004). TDP1$^{-/-}$ mice are not only hypersensitive to CPT, but also to bleomycin, which induces DSBs (Hirano *et al*, 2007; Katyal *et al*, 2007).

In recent years it has become apparent that the cellular DNA damage response (DDR) is a rich signalling network. In addition to DNA repair *per se*, this network activates cell-cycle checkpoints and modulates numerous cellular processes while the damage is being repaired (Harrison and Haber, 2006; Pommier *et al*, 2006b). The most powerful activators of the DDR are DSBs (Harrison and Haber, 2006). Primary transducers of the DSB response are the nuclear serine–threonine kinases: ATM (ataxia-telangiectasia mutated) (Shiloh, 2006; Lee and Paull, 2007), DNA-dependent protein kinase (DNA-PK) and to a certain extent, a related protein, ATR (ataxia-telangiectasia and Rad3 related) (Cimprich and Cortez, 2008). ATM is rapidly activated in response to DSB (Bakkenist and Kastan, 2003; Lee and Paull, 2007) and phosphorylates a plethora of key players operating in the DDR pathways (Shiloh, 2006; Matsuoka *et al*, 2007). DNA-PK is involved in non-homologous end-joining (NHEJ) of DSB (Weterings and Chen, 2007). Loss or inactivation of ATM leads to a severe genomic instability syndrome, ataxia-telangiectasia (A-T) that is characterized by progressive cerebellar degeneration, immunodeficiency, premature aging, gonadal dysgenesis, extreme radiosensitivity, and high incidence of lymphoreticular malignancies (Chun and Gatti, 2004).

Little is known about the regulation of TDP1. XRCC1 (X-ray cross-complementing group 1) has previously been found in association with TDP1 and has been implicated in the repair of Top1cc (Plo *et al*, 2003; El-Khamisy *et al*, 2005). XRCC1-deficient cells are hypersensitive to CPT and defective in TDP1 activity (Plo *et al*, 2003; Horton *et al*, 2008). TDP1 has been shown to interact directly with ligase IIIα (El-Khamisy *et al*, 2005), which directly binds to XRCC1 and thus could contribute to the presence of TDP1 and XRCC1 in the same repair complexes (Plo *et al*, 2003; El-Khamisy *et al*, 2005). XRCC1 functions as a scaffold protein and coordinates the assembly of base excision repair (BER) proteins (Caldecott, 2008) including polynucleotide kinase phosphatase (PNKP), which also binds directly to XRCC1 (Caldecott, 2003; Loizou *et al*, 2004; Ali *et al*, 2009) and is required to further process the DNA ends produced by TDP1 by removing the 3′ phosphate and adding a 5′ phosphate (Plo *et al*, 2003; Dexheimer *et al*, 2008).

Here, we show that TDP1 can be regulated by phosphorylation at S81 (S81) by ATM and/or DNA-PK, and we investigate the functional impact of this post-translational modification and its relationship with XRCC1.

Results

DNA damage induces phosphorylation of human TDP1 at S81

The target sites for ATM are serine or threonine residues followed by glutamine (SQ or TQ motif) (Abraham, 2004). Human TDP1 contains four SQ motifs (Figure 1A). We used a phospho-specific antibody that recognizes the epitope mg(s*)qe (the asterisk denotes phosphorylation). This antibody was raised against another ATM substrate currently under investigation, and is expected to recognize a similar epitope spanning phosphorylated S81 of TDP1. Figure 1B shows that the antibody recognizes a single band with molecular weight similar to that of TDP1 in cells treated with CPT. The specificity of the antibody for phosphorylated S81 was confirmed using ectopically expressed wild-type FLAG–TDP1 (FLAG–TDP1^{WT}) and mutated FLAG–TDP1 variants (S81A, S365A and S563A; Figure 1C). Knock down of TDP1 by siRNA abrogated the pS81-TDP1 signal in CPT-treated cells (Figure 1D), indicating the specificity of the antibody for pS81 of TDP1. Using the pS81-TDP1 antibody, we found that S81 phosphorylation was induced both by Top1cc (CPT) and ionizing radiation (Figure 1E).

TDP1 phosphorylation at S81 is associated with focal accumulation of TDP1 at DNA damage sites

To follow the subcellular distribution of pS81-TDP1 after DNA damage, we used the pS81-TDP1 antibody in confocal immunofluorescence microscopy. Following genotoxic stress, the antibody revealed nuclear foci that co-localize with γH2AX foci (Figure 2). The induction of pS81-TDP1 foci was inhibited by TDP1 siRNA knockdown (Figure 2A), indicating the specificity of the pS81-TDP1 antibody. γH2AX foci formation was increased in TDP1 siRNA knockdown cells (Figure 2A and Supplementary Figure S1A and B), consistent with the role of TDP1 in DNA repair (Plo *et al*, 2003; El-Khamisy *et al*, 2005; Miao *et al*, 2006; see also Figure 8). pS81-TDP1 foci were also induced in HCT116 cells treated with CPT and ionizing radiations (Figure 2B). In all cases pS81-TDP1 foci co-localized with γH2AX foci (Figure 2; also see Figures 3C and D). The appearance of pS81-TDP1 foci was rapid, and readily detectable after a 30-min incubation with CPT (Figure 2C). Although most Top1cc intermediates reverse within minutes after washing out CPT (Covey *et al*, 1989), pS81-TDP1 foci persisted and remained co-localized with γH2AX foci for several hours after CPT removal (Figure 2D).

Phosphorylation of TDP1 at S81 is induced both by replication- and transcription-coupled DNA damage

As TDP1 is involved in the repair of both replication- and transcription-dependent DNA damage induced by Top1cc (El-Khamisy *et al*, 2005; Miao *et al*, 2006), we tested whether pS81-TDP1 induction was replication dependent or transcription dependent. To that effect, we used the DNA polymerase inhibitor, aphidicolin (APH), to arrest replication (Furuta *et al*, 2003) and 5,6-dichlorobenzimidazole 1-β-D-ribofuranoside (DRB) to inhibit transcription (Sordet *et al*, 2009). At low-dose CPT, APH completely abrogated CPT-induced TDP1-S81 phosphorylation (Figure 3A), indicating pS81-TDP1 activation by replication-associated damage. However, at high-dose CPT (25 μM), APH or DRB alone only partially
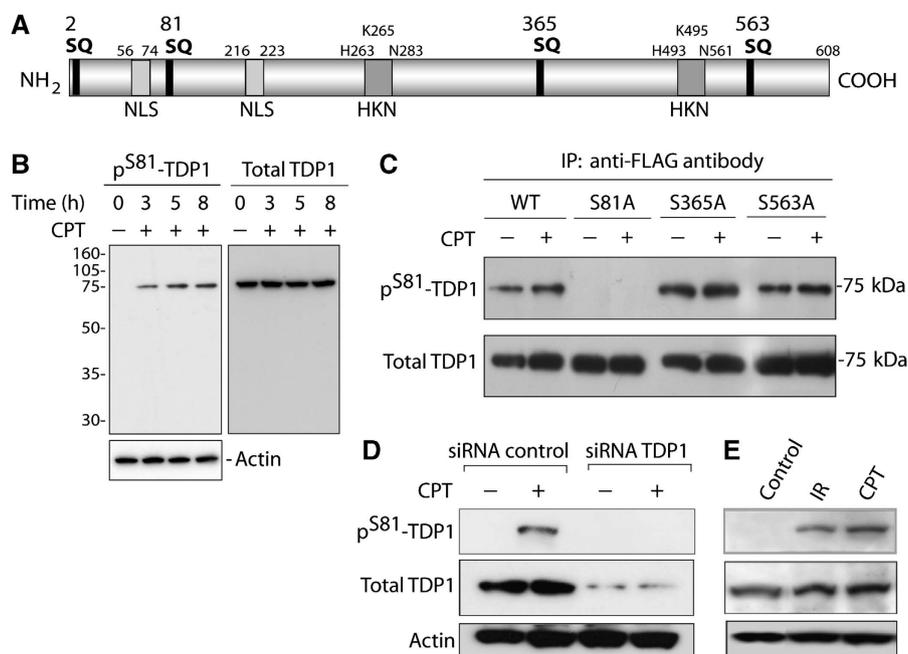
Figure 1 Human TDP1 is phosphorylated at S81 on DNA Damage. (**A**) Schematic representation of human TDP1 with the four SQ motifs. The positions of the active sites (HKN motifs) and nuclear localization sequences (NLS) are also shown. (**B**) In response to CPT treatment, the phospho-specific antibody recognizes a single band with molecular weight corresponding to TDP1. HCT116 cells were treated with 25 μM CPT for the indicated times and cellular extracts were analysed by western blotting. The blot shown on the left was stripped and re-probed with anti-TDP1 antibody (right). (**C**) Detection of pS81 by the phospho-specific antibody. Flag-tagged wild-type (WT) and mutant (S81A, S365A, and S563A) TDP1 were ectopically expressed in HCT116 cells. After treatment with 25 μM CPT for 2 h, FLAG–TDP1 was immunoprecipitated using anti-FLAG antibody and immune complexes were blotted with the anti-pS81-TDP1 antibody. The same blot was stripped and re-probed with anti-TDP1 antibody. The pS81-TDP1 signal in the untreated samples (−) is probably related to transfection. (**D**) SiRNA knockdown of TDP1 in MDA MB 231 cells abrogates the pS81-TDP1 signal on DNA damage with CPT (25 μM for 2 h), indicating the specificity of the antibody for pS81 of TDP1. (**E**) Phosphorylation of endogenous TDP1 at S81 in HCT116 cells after treatment with IR (10 Gy) and CPT (25 μM). Cells were analysed 3 h after irradiation or continuous CPT exposure.

suppressed S81-TDP1 phosphorylation, and a combination of APH and DRB was required to abrogate S81-TDP1 phosphorylation (Figure 3B).

To further demonstrate the transcriptional dependence for TDP1 phosphorylation at S81, we used non-replicating primary human lymphocytes. Figures 3C and D show the induction of pS81-TDP1 foci in CPT-treated lymphocytes. The pS81-TDP1 foci co-localized with the γH2AX foci and pre-treatment with DRB inhibited the induction of foci (Figure 3C). To confirm the occurrence of replication-independent pS81-TDP1 foci in proliferative cells, we pulse-labelled HCT116 cells with bromodeoxyuridine (BrdU), which is incorporated in replication foci selectively during S phase (Seiler *et al*, 2007), and performed co-immunostaining for pS81-TDP1 (Supplementary Figure S2). Under these conditions, CPT induced pS81-TDP1 and γH2AX foci both in replicating and non-replicating (BrdU-negative) cells. Taken together, these results indicate that both replication- and transcription-mediated DNA damages induce S81-TDP1 phosphorylation.

Phosphorylation of TDP1 on S81 is both ATM and DNA-PK dependent

To determine whether ATM and/or DNA-PK are involved in TDP1 phosphorylation at S81, we first used specific inhibitors of ATM (KU55933; ATMi) and DNA-PK (NU7441; DNA-PKi) (Hickson *et al*, 2004; Leahy *et al*, 2004). Pre-incubation with each inhibitor partially suppressed the CPT-induced TDP1-S81 phosphorylation, whereas a combination of both drugs

almost completely inhibited S81 phosphorylation (Figures 4A and B). We cannot exclude that the small residual CPT-induced pS81-TDP1 signal (Figure 4A, lane 5) could be due to ATR because ATM and ATR substrates overlap in DNA damage pathways induced by Top1cc (Furuta *et al*, 2003). ATM dependence was further examined using A-T fibroblasts. Figure 4C shows significant reduction in CPT-induced phosphorylation at S81 in A-T fibroblasts. Figure 4D shows co-localization of the pS81-TDP1 foci with activated ATM, as detected using an antibody against the ATM autophosphorylation site S1981 (Bakkenist and Kastan, 2003).

To obtain direct evidence for TDP1 phosphorylation by ATM and DNA-PK, we examined whether ATM or DNA-PK could directly phosphorylate TDP1 using *in vitro* kinase assays. Recombinant His-TDP1 (TDP1^{WT}) and the S81A mutant (TDP1^{S81A}) were used as substrates for immunoprecipitated ATM or DNA-PK. Phosphorylation of TDP1^{WT} by both kinases, but not of TDP1^{S81A} (Figures 4E and F), indicates that both ATM and DNA-PK can phosphorylate TDP1 *in vitro* at S81. S81 is phylogenetically conserved in different vertebrate species. The 'SQ' motif of human, monkey, and pig TDP1 is replaced by an 'SP' motif in rat and mouse (Supplementary Figure S3), which could be a target site for DNA-PK (O'Neill *et al*, 2000). Thus, S81 is likely to be a cellular target site for ATM and DNA-PK.

S81 phosphorylation stabilizes TDP1

Phosphorylation of downstream targets such as p53 by the DDR kinases can regulate their activity, stability, subcellular
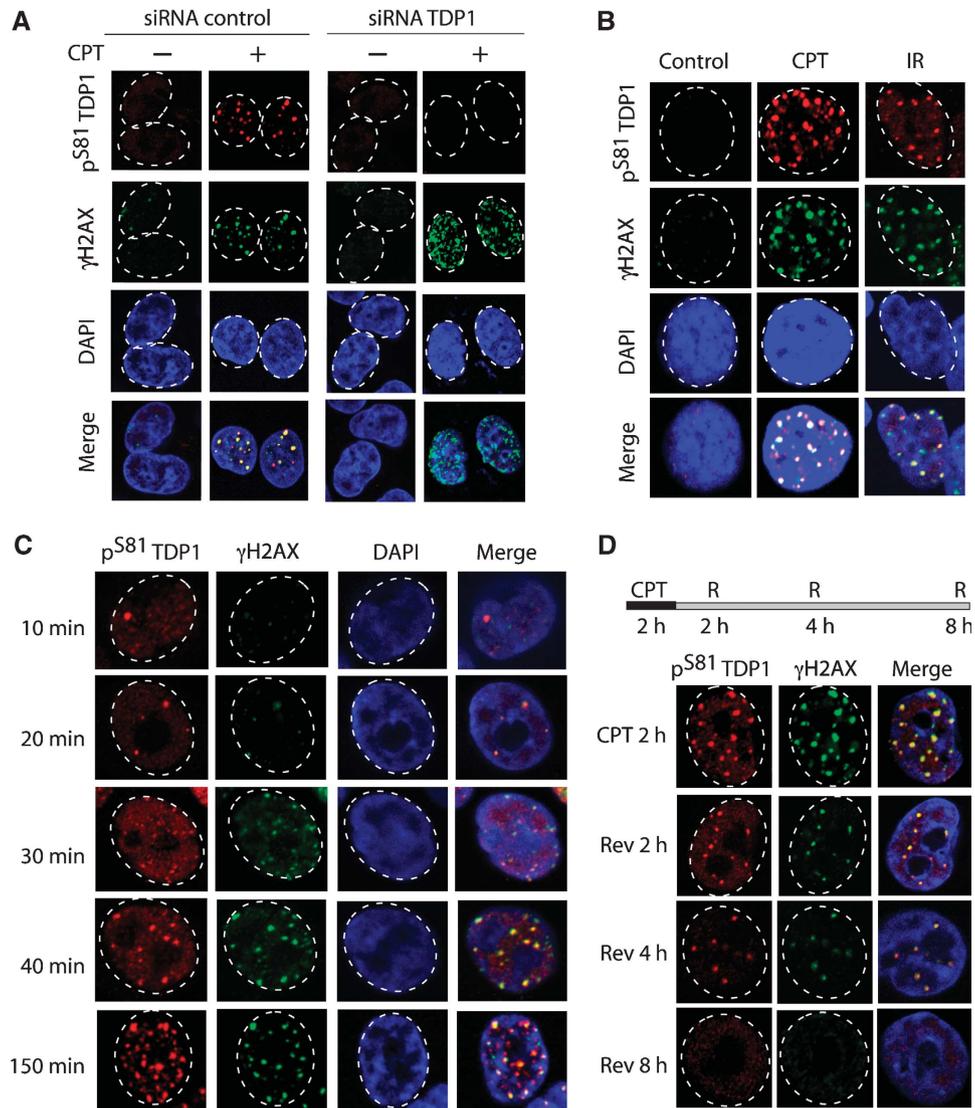
Figure 2 TDP1 phosphorylation at S81 is associated with its focal accumulation at DNA damage sites. (**A**) Immunofluorescence microscopy analysis of TDP1 knockdown cells treated with CPT (25 μM for 2 h). Focal accumulation of pS81-TDP1 and γH2AX are shown in red and green, respectively. Nuclei were stained using DAPI. Note the co-localization of pS81-TDP1 and γH2AX (merged images). (**B**) Immunofluorescence microscopy analysis of HCT116 cells treated with CPT (25 μM for 3 h) or IR (10 Gy + 3 h). Focal accumulations of pS81-TDP1 and γH2AX are shown in red and green, respectively. Nuclei were stained with DAPI. Co-localization of pS81-TDP1 and γH2AX (merged images) indicates the formation of pS81-TDP1 foci at sites of DNA damage. (**C**) Kinetics of pS81-TDP1 foci in HCT116 cells treated with CPT (25 μM). pS81-TDP1 and γH2AX foci are shown in red and green, respectively. Nuclei were stained using DAPI. (**D**) Kinetics of disappearance of pS81-TDP1 foci after CPT removal. HCT116 cells were treated with CPT (25 μM for 2 h). After CPT removal (R), cells were cultured in drug-free medium for the indicated times (indicated at the top). Nuclei are outlined in dashed white lines.

localization, or molecular interactions (Shiloh, 2006). To examine the stability of endogenous TDP1, experiments were carried out in the presence of the protein synthesis inhibitor cycloheximide (CHX). The half-life of total wild-type TDP1 was significantly prolonged in CPT-treated cells and was comparable to the half-life of pS81-TDP1 (Figures 5A and B).

Next, we measured the stability of the exogenous FLAG–TDP1^WT and the phosphomutant FLAG–TDP1^S81A polypeptides in cells treated with CPT in the presence of CHX. Figures 5C and D show the faster disappearance of the FLAG–TDP1^S81A compared with FLAG–TDP1^WT, consistent with the possibility that S81 phosphorylation stabilizes TDP1. This led us to test whether TDP1 stabilization resulted in TDP1 accumulation. Accordingly, TDP1 levels

were observed to be increased by two- to three-fold in response to CPT, and paralleled the pS81 signal. This effect was both concentration (Figures 5E and F) and time dependent (Figures 5G and H). TDP1 as well as pS81-TDP1 levels subsequently diminished by 20 h post CPT treatment (Figures 5G and H).

To determine whether TDP1 expression was also transcriptionally regulated, we measured *TDP1* mRNA expression. CPT treatment did not increase but rather decreased the *TDP1* mRNA levels (Supplementary Figure S4), which may account at least in part for the reduction of TDP1 protein levels after 20 h drug exposure. In view of the decreased stabilization of the S81A mutant, we surmise that phosphorylation of TDP1 at S81 by ATM and/or DNA-PK increases TDP1 stability.
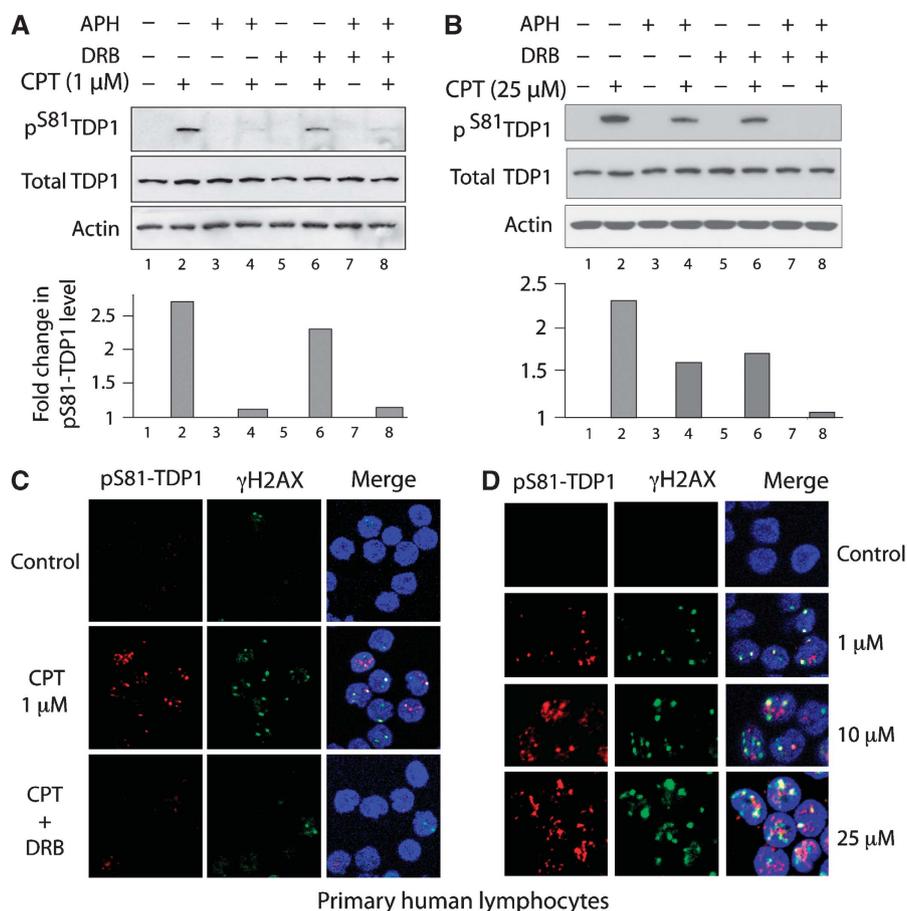
Figure 3 TDP1 phosphorylation at S81 is induced both by replication- and transcription-associated DNA damage. (**A**, **B**) Top panels: HCT116 cells were pre-treated with 1 μM aphidicolin (APH) for 15 min or 100 μM of DRB for 1 h followed by 2-h treatment with CPT at (A) low (1 μM) or (B) high concentration (25 μM) to prevent the replication- and transcription-associated DSB, respectively. Cells were examined for pS81-TDP1 and total TDP1 by western blotting. Bottom panels: densitometry analysis of pS81-TDP1 normalized against actin represents the relative level of pS81-TDP1. The numbers correspond to lanes in the top panels. (**C**) Immunofluorescence analysis of human lymphocytes treated with CPT (1 μM for 2 h). Nuclei were stained using DAPI. Lymphocytes were pre-treated with 100 μM of DRB for 1 h to arrest transcription, followed by a treatment with CPT for 2 h. Co-localization of pS81-TDP1 (red) and γH2AX (green) indicates that pS81-TDP1 foci are formed at damage sites. (**D**) Representative pictures showing dose-dependent increase of pS81-TDP1 staining with increasing concentrations of CPT for 2 h.

TDP1 phosphorylation at S81 promotes its association with XRCC1

As we previously reported that TDP1 is a part of XRCC1 complexes (Plo *et al*, 2003), we tested whether phosphorylation of TDP1 affected its interaction with XRCC1. Immunoprecipitation of ectopic FLAG–TDP1^WT or FLAG–TDP1^S81A showed that the phosphomutant TDP1^S81A was deficient in pulling down XRCC1 from CPT-treated cell extracts (Figure 6A). Thus, S81 phosphorylation seems to promote the association of TDP with XRCC1.

The XRCC1–pS81–TDP1 interaction was further examined using immunofluorescence confocal microscopy in XRCC1-deficient and XRCC1-complemented cells (Caldecott *et al*, 1995; Plo *et al*, 2003). The XRCC1-deficient Chinese hamster ovary cells showed diffuse pS81-TDP1 distribution and low levels of pS81-TDP1 focus formation in response to CPT (Figure 6B). This defect was reversed in isogenic cells stably transfected with human XRCC1, and in those cells the XRCC1 foci tended to co-localize with the pS81-TDP1 foci (Figure 6B). As CPT-induced pS81-TDP1 foci co-localized with γH2AX foci (see Figures 2 and 3), we tested whether

CPT-induced XRCC1 foci also co-localized with γH2AX foci. Figure 6C show that subsets of CPT-induced XRCC1 foci co-localize with γH2AX foci.

To further test whether S81 phosphorylation might be involved in recruiting TDP1 to the damage sites, we used laser micro-irradiation combined confocal microscopy. The induction of DNA damage by this method was confirmed by immunostaining with γH2AX antibody (Figure 7A). Laser-induced DNA damage induced endogenous TDP1-S81 phosphorylation at the γH2AX site (Figure 7A). Under similar experimental conditions, we compared the recruitment kinetics of RFP-tagged TDP1^WT and TDP1^S81A through live-cell microscopy followed by photobleaching (FRAP analysis). The fluorescence recovery of wild-type TDP1 (RFP–TDP1^WT) was fast (83–90% in 1 min) and reached maximum intensity (100%) within 5 min, whereas the fluorescence recovery of the phosphomutant TDP1^S81A was slower (Figures 7B and C). We also analysed the recruitment kinetics of TDP1 under conditions that blocked S81 phosphorylation (see Figures 4A and B). Pre-treatment with the combination of ATM and DNA-PK inhibitors slowed down the fluorescence recovery
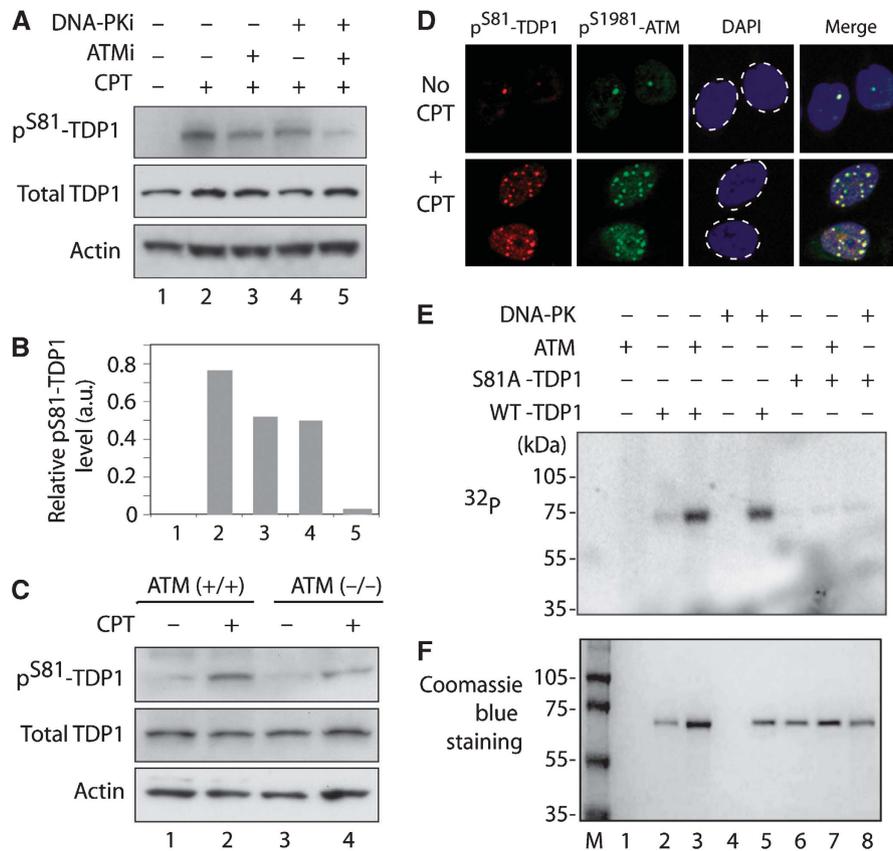
Figure 4 Both ATM and DNA-PK are involved in TDP1 phosphorylation at S81. (**A**) Effect of the ATM inhibitor KU55933 (ATMi) and of the DNA-PK inhibitor NU7441 (DNA-PKi) on TDP1 phosphorylation at S81. HCT116 cells were treated with inhibitors ($10\,\mu M$ for 1 h) before the addition of CPT ($25\,\mu M$ for 2 h). TDP1 phosphorylation (pS81-TDP1) and total TDP1 were analysed by western blotting. (**B**) Densitometry analysis of pS81-TDP1 normalized to actin under the indicated conditions. Numbers refer to the lanes in (**A**). (**C**) Defective phosphorylation of TDP1 at S81 in human A-T fibroblasts on treatment with CPT ($25\,\mu M$ for 2 h). The response of isogenic ATM-complemented A-T cells ($+/+$) is also shown. (**D**) Co-localization of pS81-TDP1 (red) and pS1981-ATM (green) foci in HCT116 cells treated with CPT ($25\,\mu M$ for 2 h). Nuclei stained with DAPI are outlined in dashed lines. (**E**) *In vitro* kinase assays with ATM or DNA-PK immunoprecipitated from HCT116 cells. The substrates were His-tagged TDP1: wild type (WT) and S81A. (**F**) Coomassie blue staining showing the amount of substrate in each reaction.

of RFP–TDP1^{WT}, mimicking the reduced recruitment of the phosphomutant TDP1^{S81A} while having no detectable impact on the fluorescence recovery of RFP–TDP1^{S81A} (Figures 7B and C). As we observed that S81 phosphorylation promotes the association of TDP with XRCC1 (Figure 6A), we next examined the recruitment of XRCC1–YFP under similar conditions. Consistent with the data obtained for RFP–TDP1^{WT} (Figure 7C), XRCC1—YFP was rapidly recruited to the DNA damage site, and showed rapid fluorescence recovery kinetics (87–95% in 1 min) with maximum intensity within 10 min (Figures 7B and D). Together, these results indicate that phosphorylation at S81 enhances the recruitment of TDP to DNA damage sites together with XRCC1.

S81-TDP1 protects cells against CPT-induced DNA damage

To investigate the biological significance of TDP1 phosphorylation at S81, we expressed the FLAG–TDP1^{S81A} and its wild-type counterpart in TDP1$^{-/-}$ MEFs (Hirano et al, 2007) and investigated the role of S81 in DNA repair using γH2AX, comet, and clonogenic survival assays.

As γH2AX is a well-characterized marker for Top1-associated DSBs (Furuta et al, 2003; Seiler et al, 2007; Sordet et al, 2009), we analysed the role of S81 in CPT-induced DSBs formation in TDP1$^{-/-}$ MEFs expressing wild-type TDP1 or

TDP1^{S81A}. Wild-type TDP1 substantially reduced γH2AX formation in transfected cells (arrows in Figure 8A and quantification in Figure 8B). In contrast, the phosphomutant TDP1^{S81A} was significantly deficient in the reduction of γH2AX compared with its wild-type counterpart (Figures 8A and B). We also found defective complementation by the S81A mutant in the γH2AX response after CPT removal (Figure 8B).

Comet assays were then used to determine whether the γH2AX results reflected differential levels of DNA breaks. Figure 8C shows that CPT-treated TDP1$^{-/-}$ MEFs expressing TDP1^{S81A} accumulate higher level of DNA breaks compared with the TDP1^{WT} counterpart. Under similar conditions, the DNA break levels of TDP1$^{-/-}$ MEFs expressing FLAG–TDP1^{WT} paralleled those of TDP1$^{+/+}$ cells (Figure 8C). We also analysed the accumulation of DNA strand breaks under conditions that blocked S81 phosphorylation. Figure 8D shows that pre-treatment with the combination of ATM and DNA-PK inhibitors induces an increase in DNA breaks in TDP1$^{-/-}$ MEFs expressing TDP1^{WT} (Figure 8C), mimicking the defect of the phosphomutant TDP1^{S81A}.

Finally, we tested the impact of the S81A mutation on cell survival. Clonogenic survival assays were performed in TDP1$^{-/-}$ MEFs transfected with the wild-type FLAG–TDP1, the phosphomutant FLAG–TDP1^{S81A} or the empty vector after
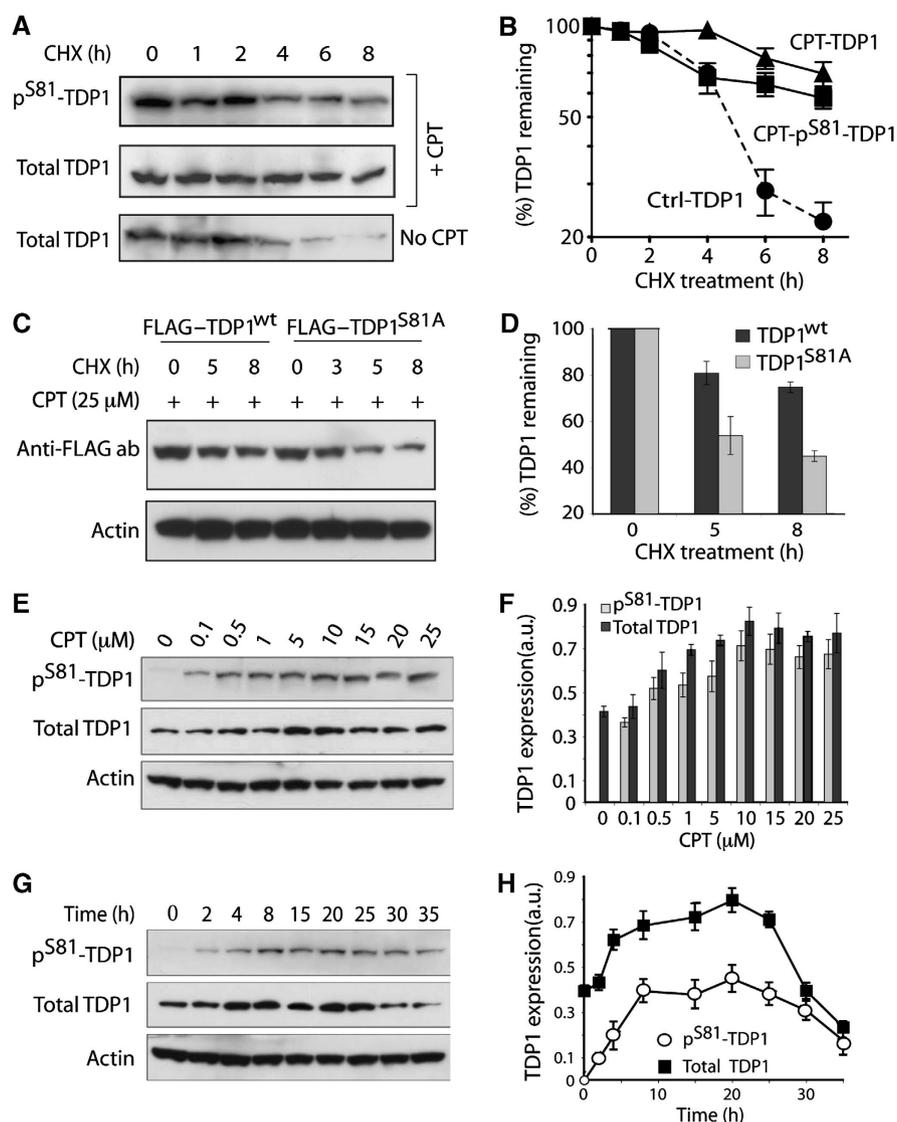
Figure 5 S81 stabilizes TDP1. (**A, B**) Increased half-life of endogenous TDP1 on CPT treatment. HCT116 cells were treated with 25 μM CPT for 2 h immediately followed by a treatment with cycloheximide (CHX) for the indicated times. Proteins (pS81-TDP1 and total TDP1) were (A) detected by western blotting (representative experiment) and (B) quantified by densitometry. (**C, D**) HCT116 cells were transfected with wild-type (WT) or the phospho-mutant S81A–FLAG-tagged TDP1, and 24 h later were treated with 25 μM CPT for 2 h immediately followed by a treatment with CHX. Protein levels were (C) determined by western blotting and (D) quantified by densitometry. (**E**) HCT116 cells were treated with increasing concentrations of CPT (0.1–25 μM) for 3 h and protein levels were analysed by western blotting (representative experiment is shown). (**F**) Densitometry analysis of pS81-TDP1 and total TDP1 normalized to actin represents the relative level of total and pS81-TDP1 after treatment with the indicated CPT concentrations. (**G**) Kinetics of TDP1 accumulation in HCT116 cells treated with 1 μM CPT for the indicated times. (**H**) Densitometry analysis of pS81-TDP1 and total TDP1 normalized to actin. Data represent the mean ± s.e. values of independent experiments.

treatment with CPT (Figure 8E). Under conditions in which transfection was similarly efficient for the FLAG–TDP1[WT] and with the FLAG–TDP1[S81A] constructs (Figure 8F), expression of the wild-type TDP1 protected TDP1^{−/−} cells significantly better than the phosphomutant (FLAG–TDP1[S81A]; Figure 8E). Similar results were observed with MTT assays (data not shown).

Together, these results provide evidence that the TDP1[S81A] is defective in terms of DNA repair and survival after CPT treatment.

Discussion

ATM is a key transducer of the DSB response (Shiloh, 2006) and DNA-PK is a major player in the NHEJ pathway of DSB repair (Weterings and Chen, 2007). In this study, we establish that both ATM and/or DNA-PK can regulate TDP1 through phosphorylation of serine 81 in response to DSBs associated with the trapping of Top1–DNA complexes and with ionizing radiations. We demonstrate that S81 phosphorylation is associated with Top1-induced DSBs, on the basis of the co-localization of pS81-TDP1 with γH2AX foci. We also show that pS81-TDP1 tends to associate with XRCC1 at those sites, which suggests an involvement of XRCC1 in the repair of Top1-linked DSBs. We show enhanced formation of DSBs in cells lacking TDP1 or expressing the TDP1[S81A] phospho-mutant, which could be a consequence of enhanced generation of DSBs and/or diminished DSB repair.

A common source of endogenous DSB is the conversion of SSB by advancing replication forks. When a replication fork
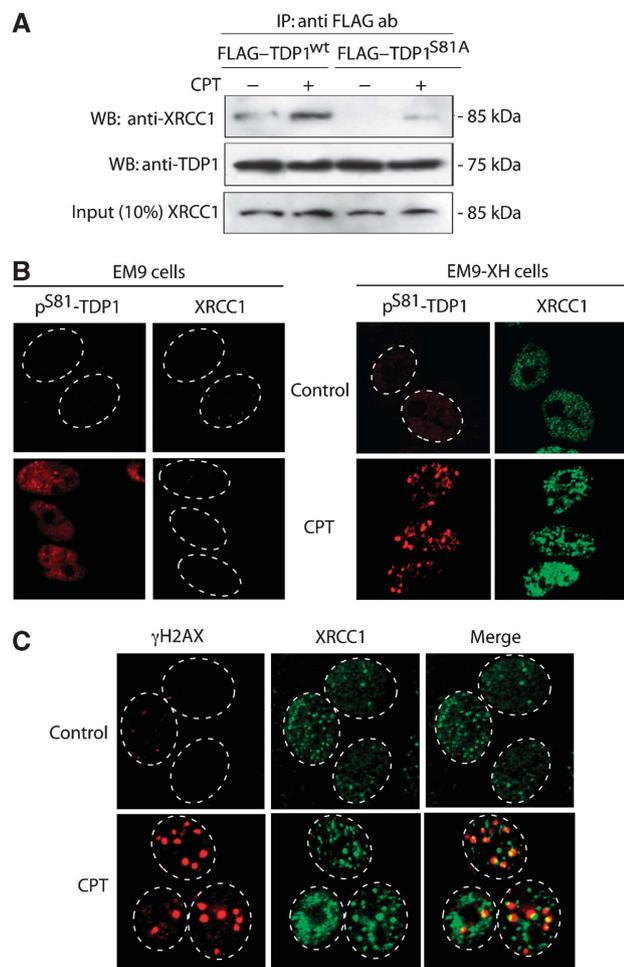
A

B

C

Figure 6 Phosphorylation of TDP1 at S81 promotes TDP1 binding to XRCC1. (**A**) Wild-type (WT) and the phospho-mutant (S81A), FLAG-tagged TDP1 were ectopically expressed in HCT116 cells. After CPT treatment (25 μM for 2 h), ectopic TDP1 was immuno-precipitated using anti-FLAG antibody and the immune complexes were blotted with anti-XRCC1 antibody. The same blot was stripped and re-probed with anti-TDP1 antibody. Aliquots (10%) of the input show the uniform presence of XRCC1 before immunoprecipitation. (**B**) XRCC1-deficient (EM9) and EM9 cells stably transfected with human XRCC1 (EM9-XH) were treated with CPT (5 μM for 2 h). Immunofluorescence microscopy shows significant reduction in pS81-TDP1 foci (red) in EM9 cells, whereas focal accumulation is restored in EM9-XH cells (green). (**C**) Immunofluorescence microscopy analysis of HCT116 cells treated with CPT (25 μM for 2 h). Focal accumulations of XRCC1 and γH2AX are shown in green and red, respectively. Nuclei are outlined in dashed white lines. Partial co-localization of XRCC1 and γH2AX (merged images) indicates subsets of CPT-induced XRCC1 foci at CPT-induced DSB sites.

proceeds toward a stalled Top1cc, the extension of the leading strand is terminated with replication fork run-off, resulting in a Top1-linked DSBs (Tsao *et al*, 1993; Strumberg *et al*, 2000). Those replication-mediated DSBs have previously been shown to induce RPA2 hyperphosphorylation and γH2AX, Chk2, and BLM nuclear foci by activation of ATM, ATR, and DNA-PK (Shao *et al*, 1999; Wang *et al*, 1999; Furuta *et al*, 2003; Rao *et al*, 2005; Takemura *et al*, 2006). The relationship between the activation of ATM and DNA-PK, and replication-mediated DSBs induced by stalled Top1cc is also evident from our results showing inhibition of TDP1 phosphorylation at S81 in cells treated with APH (Figure 3A). Our study also

shows that transcription-associated DSBs induce S81 phosphorylation. This effect tends to predominate in cancer cells at high dose of CPT, but was also detectable in non-replicating normal lymphocytes at pharmacological CPT concentrations (Figures 3C and D). These observations are in keeping with recent studies demonstrating that transcription-associated Top1cc can induce DSBs (Wu and Liu, 1997; Sordet *et al*, 2009) with activation of ATM (Sordet *et al*, 2009). Thus, our study favours the interpretation that ATM and DNA-PK are activated in response to DSBs associated with Top1cc, which then leads to phosphorylation of TDP1 at S81.

The mechanistic implications of TDP1 phosphorylation at S81 seem to involve TDP1 stability and subcellular distribution rather than a direct effect on TDP1 catalytic activity. Indeed, *in vitro* gel-based biochemical assays (Antony *et al*, 2007) with immunoprecipitates of ectopically expressed wild-type TDP1 (FLAG–TDP1[WT]) or the phosphomutant TDP1 (FLAG–TDP1[S81A]) proteins showed no detectable effect of S81 phosphorylation on the catalytic activity of TDP1 (data not shown). This finding is consistent with the fact that the N-terminal fragment, spanning positions 1–148 of TDP1, is not required for TDP1 activity *in vitro* (Interthal *et al*, 2001).

We also find that S81 phosphorylation enhances TDP1 interactions with XRCC1 (see Figure 6), and promotes the recruitment of TDP1 to DNA damage sites (see Figure 7). XRCC1 has been primarily implicated in single-strand break rejoining in the BER pathway and is devoid of enzymatic activity (Caldecott, 2003, 2008; Parsons *et al*, 2008). However, XRCC1 binds repair enzymes, including apurinic endonuclease I (APE1), poly(ADP-ribose) polymerase (PARP), ligase IIIα, pol β and PNKP (Caldecott, 2003; Loizou *et al*, 2004). XRCC1 is also known to promote the repair of Top1cc (Plo *et al*, 2003; Horton *et al*, 2008), which could be related to its interactions with PARP, PNKP, and TDP1 (Pommier *et al*, 2006a). Our results show that a subset of the CPT-induced XRCC1 foci co-localizes with γH2AX and pS81-TDP1 foci. These sites probably correspond to the small fraction of cleavage complexes that are converted into irreversible Top1–DNA complexes in association with replication (Furuta *et al*, 2003; Seiler *et al*, 2007) and transcription (Sordet *et al*, 2009). The co-localization of pS81-TDP1 with γH2AX foci is consistent with the presence of TDP1 along with XRCC1 within this subset of Top1-associated DNA damage sites. Thus, it is plausible that XRCC1 may have a specific role in the repair of lesions associated with Top1-linked DSBs (Figure 9). Whether the phosphorylation of TDP1 affects SSB as well as DSB repair is currently unclear although phosphorylation seems to be driven by DSB formation.

Earlier studies have already proposed possible involvement of XRCC1 in an alternative end-joining pathway for DSB repair (Audebert *et al*, 2004; Rosidi *et al*, 2008). XRCC1-deficient cell lines also show a significant defect in rejoining radiation-induced DSB (Nocentini, 1999), and XRCC1 depletion sensitizes cells to the DSB-inducing agent bleomycin (Rose *et al*, 2007). Two recent studies describe a potential link between the ATM–Chk2 pathway and XRCC1 by phosphorylation of XRCC1 (Chou *et al*, 2008). Furthermore, DNA-PK has been shown to interact with XRCC1 and to phosphorylate XRCC1 at serine 371 (Levy *et al*, 2006; Toulany *et al*, 2008). Thus, we conclude that the phosphorylation of TDP1 by ATM and/or DNA-PK induces the
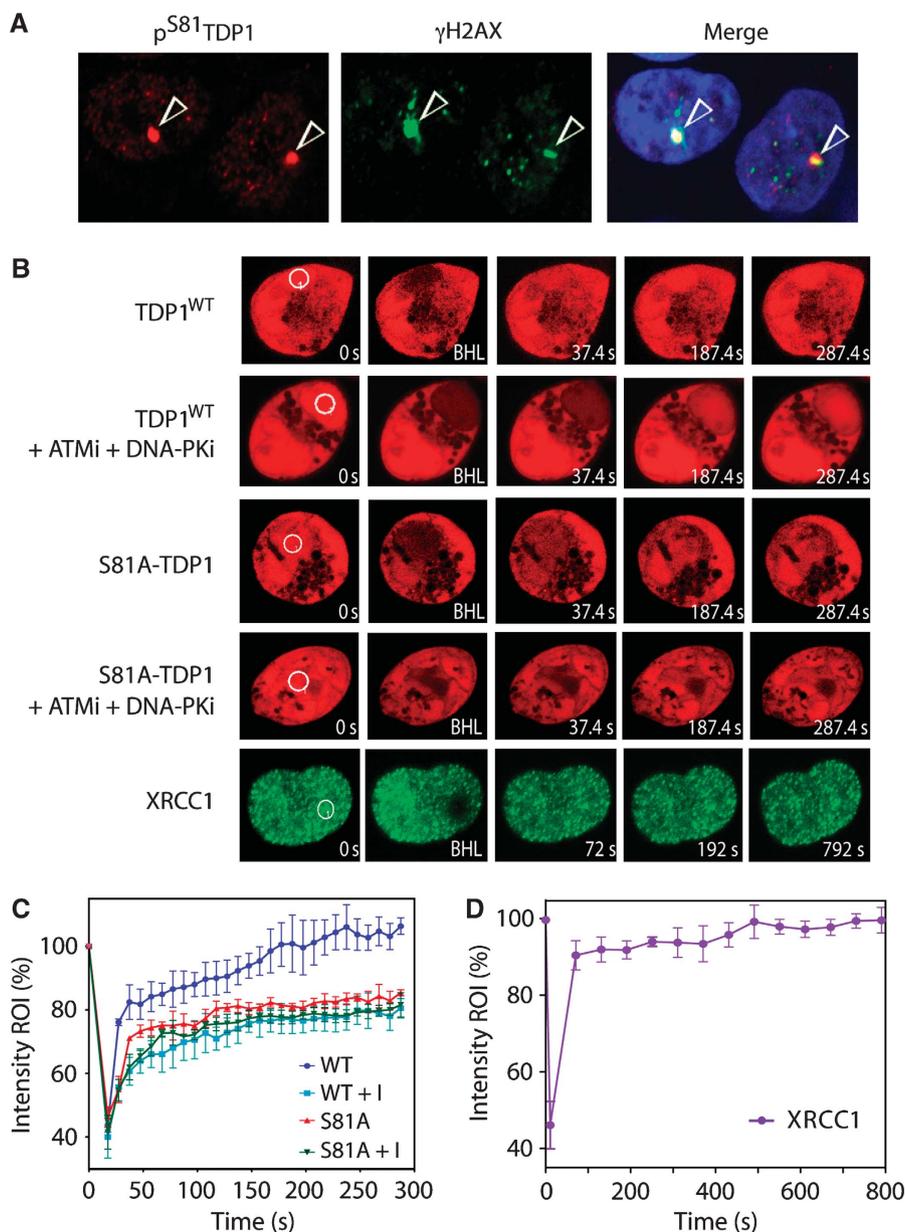
Figure 7 Recruitment of RFP–TDP1 to DNA damage sites depends on S81. (**A**) Immunochemical detection of endogenous TDP1 phosphorylation at S81 after laser-induced DNA damage. Cells were fixed after 10 min of microirradiation and were stained with anti-pS81-TDP1 (left) or γH2AX antibody (middle). Nuclei were stained using DAPI. Co-localization of pS81-TDP1 and γH2AX (merged images) indicates the accumulation of pS81-TDP1 at sites of laser-induced DNA damage sites. Arrows indicate the sites of irradiation. (**B**) Recruitment of TDP1^{WT}–RFP, phosphomutant TDP1^{S81A}–RFP, XRCC1–YFP, TDP1^{WT}–RFP, and TDP1^{S81A}–RFP, pre-treated for 1 h with both the ATM inhibitor KU55933 (ATMi, 10 μM) and the DNA-PK inhibitor NU7441 (DNA-PKi, 10 μM), were analysed by microirradiation using live-cell microscopy and photobleaching (FRAP analysis). A sub-nuclear spot indicated by a circle was bleached (BLH) for 300 ms and photographed at regular intervals of 10 s thereafter. Successive images taken for ~300 s after bleaching illustrate the level of return of fluorescence into the bleached areas. For XRCC1–YFP, images were photographed for ~800 s at intervals of 60 s. (**C**) Quantitative FRAP data of HCT 116 cells expressing TDP1^{WT}–RFP, TDP1^{WT}–RFP (ATMi + DNA-PKi) or the phosphomutant TDP1^{S81A}–RFP and TDP1^{S81A}–RFP (ATMi and DNA-PKi) ($n = 3$) showing mean curves. Error bars represent the s.e. values of the mean. (**D**) Quantitative FRAP data of HCT116 cells expressing XRCC1–YFP ($n = 5$). Error bars represent the s.e.m. values.

formation of stable TDP1 complexes with XRCC1 at Top1-linked DSB damage sites.

In summary, our study demonstrates the first post-translational modification of TDP1 in response to DNA damage. It establishes the biological significance of TDP1 phosphorylation at S81 and proposes a new post-translational regulation mechanism for TDP1 (Figure 9). Stalled Top1cc associated with DSBs activates ATM and DNA-PK that phosphorylate TDP1 at S81, stabilize TDP1, promote the binding of TDP1

with XRCC1, and facilitate the repair of Top1-induced DSBs and cell survival.

Materials and methods
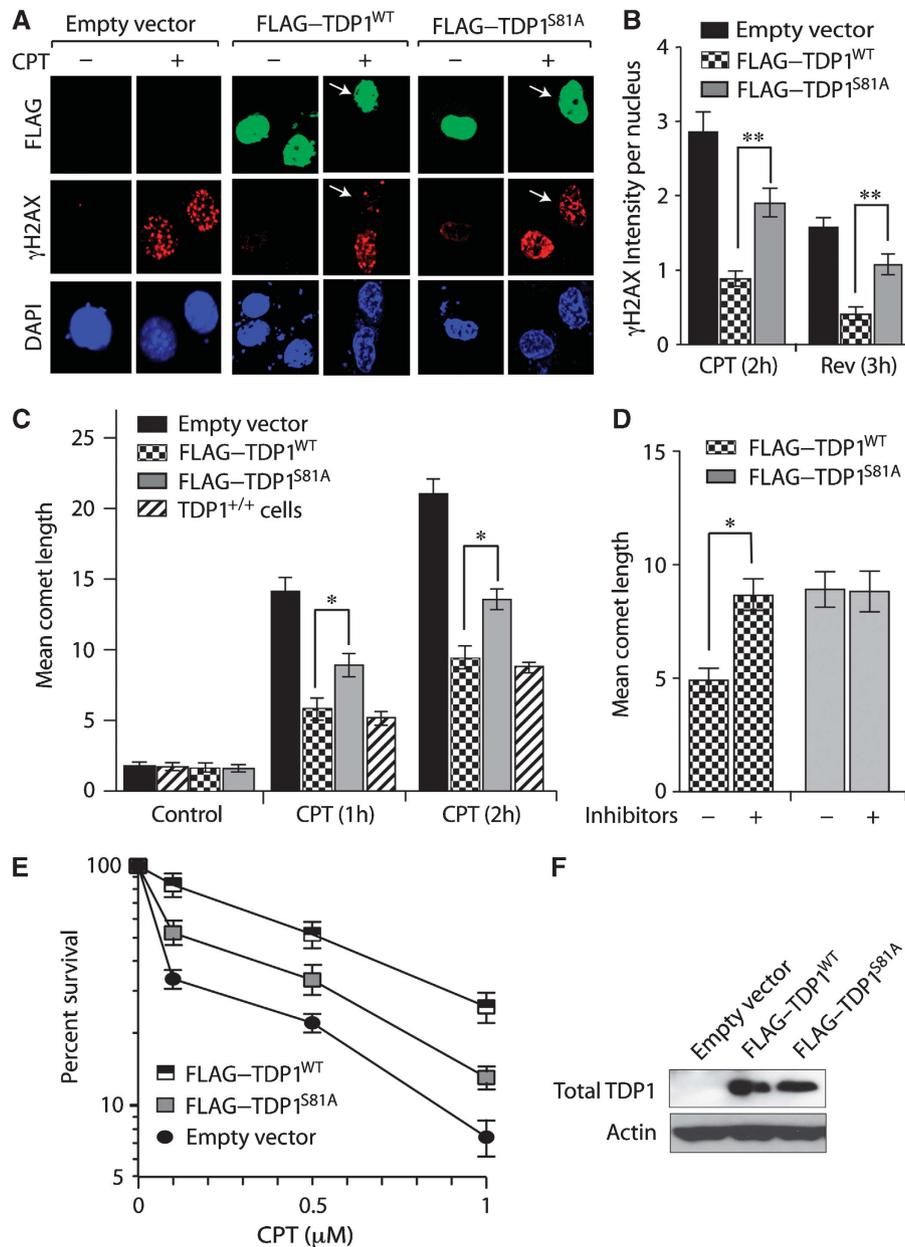
Drug and antibodies

Figure 8 S81-TDP1 promotes cell survival and DNA repair in response to CPT-induced DNA damage. (**A**) Immunofluorescence microscopy analysis for induction of γH2AX in TDP1$^{-/-}$ cells expressing FLAG–TDP1^{WT}, FLAG–TDP1^{S81A} or vector control treated with CPT (5 μM for 2 h). Representative pictures showing expression of FLAG–TDP1^{WT} or FLAG-TDP1^{S81A} detected by immunofluorescence staining with anti-FLAG antibody (green). γH2AX induction is shown in red. Cells were counterstained with DAPI to visualize nuclei. Arrows indicate the differential induction of γH2AX in TDP1$^{-/-}$ cells transfected with TDP1^{WT} or TDP1^{S81A}. The level of γH2AX is also shown in the untransfected ($-$TDP1^{WT}, $-$TDP1^{S81A}) cells in the same field 24 h after of transfection. (**B**) Quantification of γH2AX intensity per nucleus after CPT treatment (5 μM for 2 h) and 3 h after CPT removal (5 μM CPT for 2–3 h in drug-free medium) was calculated for 30–40 cells (calculated value $\pm$ s.e.). Asterisks denote significant difference (**$P<0.001$; t test). (**C**) Differential DNA strand breaks measured by alkaline comet assays in response to CPT (5 μM) in TDP1$^{-/-}$ MEFs cells expressing TDP1^{WT}, TDP1^{S81A} and empty vector or in TDP1$^{+/+}$ MEFs cells. (**D**) Effects of ATM and DNA-PK inhibitors on CPT-induced strand breaks in TDP1$^{-/-}$ MEFs cells expressing TDP1^{WT} or TDP1^{S81A}. Pretreatment with both the ATM inhibitor KU55933 (ATMi, 10 μM) and the DNA-PK inhibitor NU7441 (DNA-PKi, 10 μM) was for a duration of 1 h before the addition of CPT (5 μM) for an additional hour. Asterisks denote statistically significant difference (*$P<0.05$; t test). (**E**) Clonogenic survival of TDP1$^{-/-}$ MEFs cells expressing TDP1^{WT}, TDP1^{S81A}, or empty vector after treatment with the indicated concentrations of CPT for 24 h. Percent survival was normalized to the observed number of colonies from untreated control $\pm$ s.e. (**F**) Representative western blot showing TDP1 protein levels in TDP1$^{-/-}$ MEFs cells expressing TDP1^{WT}, TDP1^{S81A}, or empty vector 24 h after transfection.

from Sigma (St Louis, MO). The ATM inhibitor (KU55933) (Hickson *et al*, 2004) and the DNA-PK inhibitor (NU7441) (Leahy *et al*, 2004) were obtained from Kudos Pharmaceuticals (Cambridge, UK). Mouse polyclonal anti-human TDP1 (cat no. H00055775-A01) antibody was purchased from AbNova. Rabbit polyclonal TDP1 (Ab4166) and XRCC1 (Ab1838, mouse monoclonal) were obtained from Abcam (Cambridge, MA). Mouse monoclonal and rabbit polyclonal anti-γH2AX antibody were purchased from Upstate Biotechnology (Lake Placid, NY) and Novus Biologicals (Littleton, CO), respectively. Mouse monoclonal anti-Ser1981-pATM antibody was purchased from Cell Signaling Technology (Danvers, MA). Mouse monoclonal anti-Flag (M2) and anti-actin (ACTN05) antibodies were obtained from Sigma and NeoMarkers (Fremont, CA), respectively. ATM (2C1) and DNA-PK (NA57) mouse monoclonal
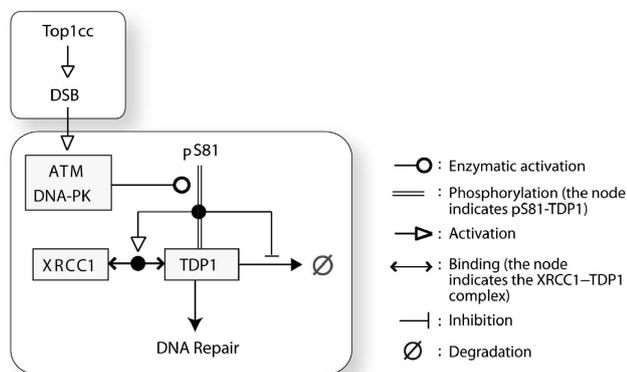
Figure 9 Schematic representation of the post-translational activation of TDP1 in response to Top1cc-induced DSBs. ATM and DNA-PK phosphorylate TDP1 at S81. S81 phosphorylation stabilizes TDP1, promotes the binding of TDP1 to XRCC1, and induces DNA repair. Symbol conventions (shown at right) are derived from Kohn's molecular interaction maps (MIMs; for further details see http://discover.nci.nih.gov).

antibodies were purchased from Santa Cruz Biotechnology (Santa Cruz, CA) and Calbiochem (EMD Biosciences, San Diego, CA), respectively. Rabbit phospho serine 81-TDP1 (pS81-TDP1) antibodies were generated by Bethyl Laboratories (Montgomery, TX) and were raised against the following phospho peptide vqksmg(ps)qeddsgn. Phospho-specific antibodies were affinity-purified and were confirmed by ELISA. Secondary antibodies: HRP-conjugated anti-rabbit IgG or anti-mouse IgG were obtained from Santa Cruz Biotechnology

Expression constructs and site-directed mutagenesis
Human FLAG–TDP1 and TDP1–DsRED fusion constructs were generated using mammalian expression vectors: pCMV-Tag2 (Stratagene, La Jolla, CA) and pDsRED1-N1 (Clontech, Palo Alto, CA), respectively, using standard PCR techniques and pET-His-TDP1 (containing full-length human TDP1; Antony *et al*, 2007) as a template. The following point mutations: FLAG–TDP1^{S81A}, FLAG–TDP1^{S365A}, FLAG–TDP1^{S563A}, TDP1^{S81A}–DsRED, and His-TDP1^{S81A} were constructed using the 'QuikChange' protocol (Stratagene, La Jolla, CA). All PCR-generated constructs were confirmed by DNA sequencing. XRCC1–YFP construct was kindly provided by Dr J Pablo Radicella (Institut de Radiobiologie Cellulaire et Moléculaire, Fontenay-aux-Roses, France).

Cell culture, treatment, and transfections
Cell cultures were maintained at 37°C under 5% CO$_2$ in Dulbecco's modified Eagle's medium containing 10% fetal calf serum (Life Technologies, Rockville, MD). The colon carcinoma cell line (HCT116) was obtained from the Developmental Therapeutics Program (NCI, NIH). TDP1$^{+/+}$ and TDP1$^{-/-}$ primary MEFs cells were a kind gift from Dr Cornelius F Boerkoel (Centre for Molecular Medicine and Therapeutics, University of British Columbia, Vancouver, British Columbia, Canada). EM9 (XRCC1-deficient Chinese hamster ovary) and EM9-XH (EM9 cells stably transfected with wild-type human XRCC1) were used as described previously (Plo *et al*, 2003). ATM-deficient cells and counterparts complemented with ATM (pEBS7 and pEBS7-YZ5, respectively; Shiloh, 2006). Human peripheral lymphocytes were obtained from the blood bank at the NIH and maintained in RPMI 1640 medium supplemented with 10% fetal calf serum. Cells were either treated with different concentration of CPT or irradiated with IR in a Mark I Irradiator. For CHX experiments, cells (60–70% confluent) were grown in six-well plates and CHX was added to a final concentration of 100 μg/ml. Plasmid DNAs were transfected with Lipofectamine 2000 (Invitrogen, Carlsbad, CA) according to the manufacturer's protocol.

siRNA transfection
Transfections were performed as described by Toulany *et al* (2008). In brief, MDA MB 231 human breast cancer cells (1.5×10^5) were transfected with control siRNA or 25 nM TDP1 siRNA (Qiagen)

using oligofectamine (Invitrogen) according to the manufacturer's protocol. Time course experiments revealed a maximum suppression of TDP1 protein at day 3 after transfection, as analysed by western blotting.

Cell extracts, immunoblotting, and immunoprecipitation
Preparation of whole cell extracts, immunoprecipitation, and immunoblotting were carried out as described previously by Plo *et al* (2003). Briefly, cells were lysed in a lysis buffer (10 mM Tris–HCl (pH 8), 150 mM NaCl, 0.1% SDS, 1% NP40, 0.5% Na-deoxycholate supplemented with complete protease inhibitors) (Roche Diagnostics, Indianapolis, IN) and phosphatase inhibitors (Phosphatase Inhibitor Cocktail 1 from Sigma). After thorough mixing and incubation at 4°C for 2 h, lysates were then centrifuged at 12 000 *g* at 4°C for 20 min. Supernatants were collected, aliquoted, and stored at −80°C.

For immunoprecipitation, cells were lysed in a lysis buffer (50 mM Tris–HCl (pH 7.4), 300 mM NaCl, 0.4% NP40, 10 mM MgCl$_2$, 0.5 mM dithiothreitol supplemented with protease and phosphatase inhibitors). Supernatants of cell lysates were obtained by centrifugation at 15 000 *g* at 4°C for 20 min and pre-cleared with 50 μl of protein A/G-PLUS agarose beads (Santa Cruz, CA). About 3–5 mg of pre-cleared lysate was incubated overnight at 4°C with indicated antibodies (2–5 μg/ml) and 50 μl of protein A/G-PLUS agarose beads. Isolated immunocomplexes were recovered by centrifugation, washed thrice with lysis buffer, and were subjected to electrophoresis on 10% Tris–glycine gels (Invitrogen) and immunoblot analysis. Immunoblottings were carried out using standard procedures, and immunoreactivity was detected through ECL chemiluminescence reaction (Amersham). Densitometric analyses of immunoblots were carried out using Image J software (NIH).

Immunocytochemistry and confocal microscopy
Immunofluorescence staining and confocal microscopy were performed as described by Takemura *et al* (2006). Briefly, cells were fixed with 4% paraformaldehyde for 10 min at room temperature. Primary antibodies against pS81-TDP1, γH2AX, pS1981-ATM, and XRCC1 were detected using anti-mouse or anti-rabbit IgG secondary antibodies labelled with Alexa 488/568 (Invitrogen). Cells were mounted in anti-fade solution with DAPI (Vector Laboratories, Burlingame, CA) and examined using a laser scanning confocal microscope (Zeiss LSM510) with a ×63 oil objective. Images were collected and processed using the Zeiss AIM software and sized in Adobe Photoshop 7.0. The γH2AX intensity per nucleus was determined with Adobe Photoshop 7.0 by measuring the fluorescence intensities normalized to the number of cell count.

In vitro kinase assays
For *in vitro* phosphorylation assays, ATM and DNA-PK were immunoprecipitated and incubated with bacterially expressed and purified His-TDP1^{WT} or His-TDP1^{S81A} proteins (1.5 μg) as described by Antony *et al* (2007). Kinase reactions were carried out as described by Canman *et al* (1998) using kinase buffer (10 mM HEPES (pH 7.5), 50 mM glycerophosphate, 50 mM NaCl, 10 mM MgCl$_2$, 10 mM MnCl$_2$, and 1 mM DTT) containing 5 μM cold ATP and 10 μCi [γ-32P] ATP at 30°C. Reactions were stopped after 30 min by adding 2× SDS loading buffer (Invitrogen). After separation by SDS–PAGE, gels were fixed, dried, and visualized using a phosphoimager (Molecular Dynamics, Sunnyvale, CA).

Clonogenic and alkaline COMET assays
TDP1$^{-/-}$ MEFs cells (2×10^6) were separately transfected with 50 μg of plasmid DNA (FLAG–TDP1^{WT}, FLAG–TDP1^{S81A}, or vector control) using Lipofectamine 2000 (Invitrogen) according to manufacturer's protocol. After 24 h, protein expressions were determined by western blot analysis. After 24-h treatment with CPT (0.1, 0.5, and 1 μM), cells were trypsinized, washed in PBS, and seeded in triplicate at a density of 500 cells per well in six-well plates. Colonies were allowed to grow for 10–12 days and visualized after washing with PBS, fixation in methanol for 30 min, washing again with PBS, and staining with 0.05% methylene blue for 30 min. Percent survival was normalized to the observed number of colonies generated from untreated cells.

To compare the levels of DNA damage in TDP1$^{-/-}$ MEFs cell transfected with FLAG–TDP1^{WT}, FLAG–TDP1^{S81A} and vector control

or in TDP1$^{+/+}$ cells, they were subjected to alkaline comet assays according to the manufacturer's instructions (Trevigen, Gaithesburg, MD). Briefly, after treatment with 5 μM CPT, cells were collected and mixed with low melting agarose. Slides were immersed in lysis solution at 4°C for 1 h. After a rinse with deionized water, slides were immersed in a 4°C alkaline solution (50 mM NaOH, 1 mM EDTA, and 1% dimethyl sulfoxide) for 1 h. Electrophoresis was carried out at a constant voltage of 25 V for 30 min at 4°C. After electrophoresis, slides were neutralized in 0.4 M Tris–HCl (pH 7.5), dehydrated in ice-cold 70% ethanol for 5 min, and air-dried. DNA was stained with SYBR Green I stain. The relative length and intensity of SYBR Green-stained DNA, tails to heads, is proportional to the amount of DNA damage present in the individual nucleus. Comet length was measured using the TriTek Comet Score software (TriTek Corp, Sumerduck, VA) and was scored for at least 50 cells. Distributions of comet lengths were compared using the Student *t*-test.

Live-cell microscopy and photobleaching experiments

Live-cell imaging, microirradiation, and photobleaching experiments were carried out as described in previous studies (Lukas *et al*, 2004; Mortusewicz and Leonhardt, 2007) using a Zeiss LSM510 confocal laser-scanning microscope equipped with a UV-laser and ×63/1.4 NA oil objective (Carl Zeiss MicroImaging). Fluorophores were excited using a 488/514-nm argon laser line and a 561-nm HeNe laser line. The microscope was equipped with a heated environmental chamber set to 37°C. FRAP analysis was carried out with living HCT116 cells grown on chamber cover glass (Nalge Nunc International, Naperville, IL). Cells were transfected with various RFP or YFP fusion proteins and mounted on an incubation chamber filled with medium 24 h after transfection.

For FRAP analysis, a subnuclear spot was bleached for 300 ms at highest intensity of an argon laser line (488/514 nm for YFP) or a 561-nm HeNe laser line (for RFP) adapted to the fluorescent protein of interest. DNA damage was carried out with a UV laser set to 50% transmission. For imaging, the laser power was attenuated to 0.1% of the bleach intensity. Subsequently, the recovery of fluorescence in the spot was monitored at 10-s intervals for ~300 s. For XRCC1–YFP, after bleach (BLH), images were photographed for ~800 s at 60-s intervals. Relative fluorescence intensities of the bleached region were corrected for background. To show the FRAP curves, the fluorescence signal measured in a region of interest (ROI) was individually normalized to the prebleach signal in the ROI according to the following equation: $ROI = (I_t - I_{bg})/(I_o - I_{bg}) \times 100$, where I_o is the intensity in the ROI during prebleaching, I_t is the intensity in the ROI at time point t, and I_{bg} is the background signal determined in a region outside of the cell nucleus.

Supplementary data

Supplementary data are available at *The EMBO Journal* Online (http://www.embojournal.org).

Acknowledgements

Conflict of interest

The authors declare that they have no conflict of interest.

References

Abraham RT (2004) PI 3-kinase-related kinases: 'big' players in stress-induced signaling pathways. *DNA Repair (Amst)* **3**: 883–887

Ali AA, Jukes RM, Pearl LH, Oliver AW (2009) Specific recognition of a multiply phosphorylated motif in the DNA repair scaffold XRCC1 by the FHA domain of human PNK. *Nucleic Acids Res* **37**: 1701–1712

Antony S, Marchand C, Stephen AG, Thibaut L, Agama KK, Fisher RJ, Pommier Y (2007) Novel high-throughput electrochemiluminescent assay for identification of human tyrosyl-DNA phosphodiesterase (Tdp1) inhibitors and characterization of furamidine (NSC 305831) as an inhibitor of Tdp1. *Nucleic Acids Res* **35**: 4474–4484

Audebert M, Salles B, Calsou P (2004) Involvement of poly(ADP-ribose) polymerase-1 and XRCC1/DNA ligase III in an alternative route for DNA double-strand breaks rejoining. *J Biol Chem* **279**: 55117–55126

Bakkenist CJ, Kastan MB (2003) DNA damage activates ATM through intermolecular autophosphorylation and dimer dissociation. *Nature* **421**: 499–506

Barthelmes HU, Habermeyer M, Christensen MO, Mielke C, Interthal H, Pouliot JJ, Boege F, Marko D (2004) TDP1 overexpression in human cells counteracts DNA damage mediated by topoisomerases I and II. *J Biol Chem* **279**: 55618–55625

Caldecott KW (2003) XRCC1 and DNA strand break repair. *DNA Repair (Amst)* **2**: 955–969

Caldecott KW (2008) Single-strand break repair and genetic disease. *Nat Rev Genet* **9**: 619–631

Caldecott KW, Tucker JD, Stanker LH, Thompson LH (1995) Characterization of the XRCC1–DNA ligase III complex *in vitro* and its absence from mutant hamster cells. *Nucleic Acids Res* **23**: 4836–4843

Canman CE, Lim DS, Cimprich KA, Taya Y, Tamai K, Sakaguchi K, Appella E, Kastan MB, Siliciano JD (1998) Activation of the ATM kinase by ionizing radiation and phosphorylation of p53. *Science* **281**: 1677–1679

Champoux JJ (2001) DNA topoisomerases: structure, function, and mechanism. *Annu Rev Biochem* **70**: 369–413

Chou WC, Wang HC, Wong FH, Ding SL, Wu PE, Shieh SY, Shen CY (2008) Chk2-dependent phosphorylation of XRCC1 in the DNA damage response promotes base excision repair. *EMBO J* **27**: 3140–3150

Chun HH, Gatti RA (2004) Ataxia-telangiectasia, an evolving phenotype. *DNA Repair (Amst)* **3**: 1187–1196

Cimprich KA, Cortez D (2008) ATR: an essential regulator of genome integrity. *Nat Rev Mol Cell Biol* **9**: 616–627

Covey JM, Jaxel C, Kohn KW, Pommier Y (1989) Protein-linked DNA strand breaks induced in mammalian cells by camptothecin, an inhibitor of topoisomerase I. *Cancer Res* **49**: 5016–5022

Dexheimer TS, Antony S, Marchand C, Pommier Y (2008) Tyrosyl-DNA phosphodiesterase as a target for anticancer therapy. *Anticancer Agents Med Chem* **8**: 381–389

El-Khamisy SF, Saifi GM, Weinfeld M, Johansson F, Helleday T, Lupski JR, Caldecott KW (2005) Defective DNA single-strand break repair in spinocerebellar ataxia with axonal neuropathy-1. *Nature* **434**: 108–113

Furuta T, Takemura H, Liao ZY, Aune GJ, Redon C, Sedelnikova OA, Pilch DR, Rogakou EP, Celeste A, Chen HT, Nussenzweig A, Aladjem MI, Bonner WM, Pommier Y (2003) Phosphorylation of histone H2AX and activation of Mre11, Rad50, and Nbs1 in response to replication-dependent DNA double-strand breaks induced by mammalian DNA topoisomerase I cleavage complexes. *J Biol Chem* **278**: 20303–20312

Harrison JC, Haber JE (2006) Surviving the breakup: the DNA damage checkpoint. *Annu Rev Genet* **40**: 209–235

Hawkins AJ, Subler MA, Akopiants K, Wiley JL, Taylor SM, Rice AC, Windle JJ, Valerie K, Povirk LF (2009) *In vitro* complementation of Tdp1 deficiency indicates a stabilized enzyme–DNA adduct from tyrosyl but not glycolate lesions as a consequence of the SCAN1 mutation. *DNA Repair (Amst)* **8**: 654–663

Hickson I, Zhao Y, Richardson CJ, Green SJ, Martin NM, Orr AI, Reaper PM, Jackson SP, Curtin NJ, Smith GC (2004) Identification and characterization of a novel and specific inhibitor of the ataxia-telangiectasia mutated kinase ATM. *Cancer Res* **64**: 9152–9159

Hirano R, Interthal H, Huang C, Nakamura T, Deguchi K, Choi K, Bhattacharjee MB, Arimura K, Umehara F, Izumo S, Northrop JL,

Salih MA, Inoue K, Armstrong DL, Champoux JJ, Takashima H, Boerkoel CF (2007) Spinocerebellar ataxia with axonal neuropathy: consequence of a Tdp1 recessive neomorphic mutation? *EMBO J* **26:** 4732–4743

Horton JK, Watson M, Stefanick DF, Shaughnessy DT, Taylor JA, Wilson SH (2008) XRCC1 and DNA polymerase beta in cellular protection against cytotoxic DNA single-strand breaks. *Cell Res* **18:** 48–63

Hsiang YH, Hertzberg R, Hecht S, Liu LF (1985) Camptothecin induces protein-linked DNA breaks via mammalian DNA topoisomerase I. *J Biol Chem* **260:** 14873–14878

Interthal H, Chen HJ, Champoux JJ (2005a) Human Tdp1 cleaves a broad spectrum of substrates, including phosphoamide linkages. *J Biol Chem* **280:** 36518–36528

Interthal H, Chen HJ, Kehl-Fie TE, Zotzmann J, Leppard JB, Champoux JJ (2005b) SCAN1 mutant Tdp1 accumulates the enzyme—DNA intermediate and causes camptothecin hypersensitivity. *EMBO J* **24:** 2224–2233

Interthal H, Pouliot JJ, Champoux JJ (2001) The tyrosyl-DNA phosphodiesterase Tdp1 is a member of the phospholipase D superfamily. *Proc Natl Acad Sci USA* **98:** 12009–12014

Katyal S, el-Khamisy SF, Russell HR, Li Y, Ju L, Caldecott KW, McKinnon PJ (2007) TDP1 facilitates chromosomal single-strand break repair in neurons and is neuroprotective *in vivo*. *EMBO J* **26:** 4720–4731

Leahy JJ, Golding BT, Griffin RJ, Hardcastle IR, Richardson C, Rigoreau L, Smith GC (2004) Identification of a highly potent and selective DNA-dependent protein kinase (DNA-PK) inhibitor (NU7441) by screening of chromenone libraries. *Bioorg Med Chem Lett* **14:** 6083–6087

Lee JH, Paull TT (2007) Activation and regulation of ATM kinase activity in response to DNA double-strand breaks. *Oncogene* **26:** 7741–7748

Levy N, Martz A, Bresson A, Spenlehauer C, de Murcia G, Menissier-de Murcia J (2006) XRCC1 is phosphorylated by DNA-dependent protein kinase in response to DNA damage. *Nucleic Acids Res* **34:** 32–41

Liu LF, Desai SD, Li TK, Mao Y, Sun M, Sim SP (2000) Mechanism of action of camptothecin. *Ann NY Acad Sci* **922:** 1–10

Loizou JI, El-Khamisy SF, Zlatanou A, Moore DJ, Chan DW, Qin J, Sarno S, Meggio F, Pinna LA, Caldecott KW (2004) The protein kinase CK2 facilitates repair of chromosomal DNA single-strand breaks. *Cell* **117:** 17–28

Lukas C, Melander F, Stucki M, Falck J, Bekker-Jensen S, Goldberg M, Lerenthal Y, Jackson SP, Bartek J, Lukas J (2004) Mdc1 couples DNA double-strand break recognition by Nbs1 with its H2AX-dependent chromatin retention. *EMBO J* **23:** 2674–2683

Matsuoka S, Ballif BA, Smogorzewska A, McDonald III ER, Hurov KE, Luo J, Bakalarski CE, Zhao Z, Solimini N, Lerenthal Y, Shiloh Y, Gygi SP, Elledge SJ (2007) ATM and ATR substrate analysis reveals extensive protein networks responsive to DNA damage. *Science* **316:** 1160–1166

Miao ZH, Agama K, Sordet O, Povirk L, Kohn KW, Pommier Y (2006) Hereditary ataxia SCAN1 cells are defective for the repair of transcription-dependent topoisomerase I cleavage complexes. *DNA Repair (Amst)* **5:** 1489–1494

Mortusewicz O, Leonhardt H (2007) XRCC1 and PCNA are loading platforms with distinct kinetic properties and different capacities to respond to multiple DNA lesions. *BMC Mol Biol* **8:** 81

Nitiss KC, Malik M, He X, White SW, Nitiss JL (2006) Tyrosyl-DNA phosphodiesterase (Tdp1) participates in the repair of Top2-mediated DNA damage. *Proc Natl Acad Sci USA* **103:** 8953–8958

Nocentini S (1999) Rejoining kinetics of DNA single- and double-strand breaks in normal and DNA ligase-deficient cells after exposure to ultraviolet C and gamma radiation: an evaluation of ligating activities involved in different DNA repair processes. *Radiat Res* **151:** 423–432

O'Neill T, Dwyer AJ, Ziv Y, Chan DW, Lees-Miller SP, Abraham RH, Lai JH, Hill D, Shiloh Y, Cantley LC, Rathbun GA (2000) Utilization of oriented peptide libraries to identify substrate motifs selected by ATM. *J Biol Chem* **275:** 22719–22727

Parsons JL, Tait PS, Finch D, Dianova II, Allinson SL, Dianov GL (2008) CHIP-mediated degradation and DNA damage-dependent stabilization regulate base excision repair proteins. *Mol Cell* **29:** 477–487

Plo I, Liao ZY, Barcelo JM, Kohlhagen G, Caldecott KW, Weinfeld M, Pommier Y (2003) Association of XRCC1 and tyrosyl DNA phosphodiesterase (Tdp1) for the repair of topoisomerase I-mediated DNA lesions. *DNA Repair (Amst)* **2:** 1087–1100

Pommier Y (2006) Topoisomerase I inhibitors: camptothecins and beyond. *Nat Rev Cancer* **6:** 789–802

Pommier Y, Barcelo JM, Rao VA, Sordet O, Jobson AG, Thibaut L, Miao ZH, Seiler JA, Zhang H, Marchand C, Agama K, Nitiss JL, Redon C (2006a) Repair of topoisomerase I-mediated DNA damage. *Prog Nucleic Acid Res Mol Biol* **81:** 179–229

Pommier Y, Weinstein JN, Aladjem MI, Kohn KW (2006b) Chk2 molecular interaction map and rationale for Chk2 inhibitors. *Clin Cancer Res* **12:** 2657–2661

Pouliot JJ, Robertson CA, Nash HA (2001) Pathways for repair of topoisomerase I covalent complexes in *Saccharomyces cerevisiae*. *Genes Cells* **6:** 677–687

Pouliot JJ, Yao KC, Robertson CA, Nash HA (1999) Yeast gene for a Tyr-DNA phosphodiesterase that repairs topoisomerase I complexes. *Science* **286:** 552–555

Pourquier P, Pommier Y (2001) Topoisomerase I-mediated DNA damage. *Adv Cancer Res* **80:** 189–216

Rao VA, Fan AM, Meng L, Doe CF, North PS, Hickson ID, Pommier Y (2005) Phosphorylation of BLM, dissociation from topoisomerase IIIalpha, and colocalization with gamma-H2AX after topoisomerase I-induced replication damage. *Mol Cell Biol* **25:** 8925–8937

Rose JL, Reeves KC, Likhotvorik RI, Hoyt DG (2007) Base excision repair proteins are required for integrin-mediated suppression of bleomycin-induced DNA breakage in murine lung endothelial cells. *J Pharmacol Exp Ther* **321:** 318–326

Rosidi B, Wang M, Wu W, Sharma A, Wang H, Iliakis G (2008) Histone H1 functions as a stimulatory factor in backup pathways of NHEJ. *Nucleic Acids Res* **36:** 1610–1623

Seiler JA, Conti C, Syed A, Aladjem MI, Pommier Y (2007) The intra-S-phase checkpoint affects both DNA replication initiation and elongation: single-cell and -DNA fiber analyses. *Mol Cell Biol* **27:** 5806–5818

Shao RG, Cao CX, Zhang H, Kohn KW, Wold MS, Pommier Y (1999) Replication-mediated DNA damage by camptothecin induces phosphorylation of RPA by DNA-dependent protein kinase and dissociates RPA–DNA-PK complexes. *EMBO J* **18:** 1397–1406

Shiloh Y (2006) The ATM-mediated DNA-damage response: taking shape. *Trends Biochem Sci* **31:** 402–410

Sordet O, Redon CE, Guirouilh-Barbat J, Smith S, Solier S, Douarre C, Conti C, Nakamura AJ, Das BB, Nicolas E, Kohn KW, Bonner WM, Pommier Y (2009) Ataxia telangiectasia mutated activation by transcription- and topoisomerase I-induced DNA double-strand breaks. *EMBO Rep* **10:** 887–893

Staker BL, Feese MD, Cushman M, Pommier Y, Zembower D, Stewart L, Burgin AB (2005) Structures of three classes of anticancer agents bound to the human topoisomerase I–DNA covalent complex. *J Med Chem* **48:** 2336–2345

Strumberg D, Pilon AA, Smith M, Hickey R, Malkas L, Pommier Y (2000) Conversion of topoisomerase I cleavage complexes on the leading strand of ribosomal DNA into 5′-phosphorylated DNA double-strand breaks by replication runoff. *Mol Cell Biol* **20:** 3977–3987

Takashima H, Boerkoel CF, John J, Saifi GM, Salih MA, Armstrong D, Mao Y, Quiocho FA, Roa BB, Nakagawa M, Stockton DW, Lupski JR (2002) Mutation of TDP1, encoding a topoisomerase I-dependent DNA damage repair enzyme, in spinocerebellar ataxia with axonal neuropathy. *Nat Genet* **32:** 267–272

Takemura H, Rao VA, Sordet O, Furuta T, Miao ZH, Meng L, Zhang H, Pommier Y (2006) Defective Mre11-dependent activation of Chk2 by ataxia telangiectasia mutated in colorectal carcinoma cells in response to replication-dependent DNA double strand breaks. *J Biol Chem* **281:** 30814–30823

Toulany M, Dittmann K, Fehrenbacher B, Schaller M, Baumann M, Rodemann HP (2008) PI3K-Akt signaling regulates basal, but MAP-kinase signaling regulates radiation-induced XRCC1 expression in human tumor cells *in vitro*. *DNA Repair (Amst)* **7:** 1746–1756

Tsao YP, Russo A, Nyamuswa G, Silber R, Liu LF (1993) Interaction between replication forks and topoisomerase I-DNA cleavable complexes: studies in a cell-free SV40 DNA replication system. *Cancer Res* **53:** 5908–5914

Wang JC (2002) Cellular roles of DNA topoisomerases: a molecular perspective. *Nat Rev Mol Cell Biol* **3:** 430–440

Wang Y, Zhou XY, Wang H, Huq MS, Iliakis G (1999) Roles of replication protein A and DNA-dependent protein kinase in the

regulation of DNA replication following DNA damage. *J Biol Chem* **274:** 22060–22064

Weterings E, Chen DJ (2007) DNA-dependent protein kinase in nonhomologous end joining: a lock with multiple keys? *J Cell Biol* **179:** 183–186

Wu J, Liu LF (1997) Processing of topoisomerase I cleavable complexes into DNA damage by transcription. *Nucleic Acids Res* **25:** 4181–4186

Yang SW, Burgin Jr AB, Huizenga BN, Robertson CA, Yao KC, Nash HA (1996) A eukaryotic enzyme that can disjoin dead-end covalent complexes between DNA and type I topoisomerases. *Proc Natl Acad Sci USA* **93:** 11534–11539

Zhou T, Akopiants K, Mohapatra S, Lin PS, Valerie K, Ramsden DA, Lees-Miller SP, Povirk LF (2009) Tyrosyl-DNA phosphodiesterase and the repair of 3′-phosphoglycolate-terminated DNA double-strand breaks. *DNA Repair (Amst)* **8:** 901–911

Zhou T, Lee JW, Tatavarthi H, Lupski JR, Valerie K, Povirk LF (2005) Deficiency in 3′-phosphoglycolate processing in human cells with a hereditary mutation in tyrosyl-DNA phosphodiesterase (TDP1). *Nucleic Acids Res* **33:** 289–297